# Modified Version of the MIT Rutherford Scattering Apparatus for Use in Advanced Undergraduate Laboratories

JAMES A. EARL*
*School of Physics, University of Minnesota, Minneapolis, Minnesota*
(Received 5 February 1964; in final form, 16 December 1965)

Modifications of the MIT Rutherford Scattering Apparatus (Apparatus Drawings Project No. 16) are described. These include (1) use of a self-contained circuit for amplifying, analyzing, and counting pulses from the scintillation detector and (2) interchangeable foil holders which aid in the determination of background effects and which permit studies of scattering from various foils to be made. A description of the experiment performed by students at the University of Minnesota is given.

FOR the past two years, physics students at the University of Minnesota enrolled in the senior atomic and nuclear physics laboratory and in the sophomore honors physics laboratory have performed an experiment on Rutherford scattering using apparatus based on the MIT design described in Apparatus Drawings Project No. 16.[1] In both of the above courses, fairly elaborate experiments are done in great detail and at a rather leisurely pace—completion of one experiment normally takes two to four 3-hour laboratory periods. Considerable elaboration of the original MIT design (a simple one intended for a laboratory of an entirely different nature and adapted for mass production) was necessary to modify it for use in the Minnesota laboratories. These modifications, which include an amplifier–discriminator scaler circuit and an interchangeable foil holder permitting the use of a variety of scattering foils, have proved so satisfactory in actual use that it seemed worthwhile to describe them here. The main advantage of the present apparatus over the simpler MIT version is that it allows students to obtain accurate measurements of the Rutherford-scattering cross section which are suitable for comparison with theoretical formulas.[2] To obtain quantitative results, the effects of scattering at the walls of the chamber and of energy loss in the scattering foil must be taken into account. Since the corrections for these effects are neither small nor straightforward, it seems appropriate to present here a fairly complete account of the procedures followed by students at Minnesota.

## THE APPARATUS

The detector chassis, whose schematic is shown in Fig. 1, includes all electronics needed to amplify, analyze, and count the pulses coming from the scintillation counter as well as a high-voltage power supply for the photomultiplier. All this is mounted on a standard 17-in.×8-in.×3-in. chassis with 19-in.×8-in. panel (see Fig. 2); a single coaxial cable going to the photomultiplier head carries both signals and high voltage. Standard (but somewhat out of date) vacuum-tube circuits traditionally employed in nuclear research were chosen in order to give students some familiarity with their use and to ensure reliable operation. Since the detailed operation of these circuits is described elsewhere,[3] only the following general comments need be made here.

The maximum gain and range of gain control (in approximate factors of two) of the amplifier are adequate to compensate for normally encountered variations in the sensitivity of the scintillation counter which arise from lack of uniformity among photomultiplier tubes and crystals. (The ZnS phosphor of the MIT unit was replaced with a CsI crystal.)

The integral discriminator which follows the amplifier selects for counting only those pulses whose maximum height exceeds an adjustable level set by the triggering-level control. Pulse-height information obtained with the aid of this

* Present address: Department of Physics and Astronomy, University of Maryland, College Park, Maryland.
[1] R. G. Marcley, *Apparatus Drawings Project* (Plenum Press, Inc., New York, 1962).
[2] R. D. Evans, *The Atomic Nucleus* (McGraw-Hill Book Co., Inc., New York, 1955), pp. 838–851, 819–827.
[3] W. C. Elmore and M. L. Sands, *Electronics: Experimental Techniques* (McGraw-Hill Book Co., Inc., New York, 1949).

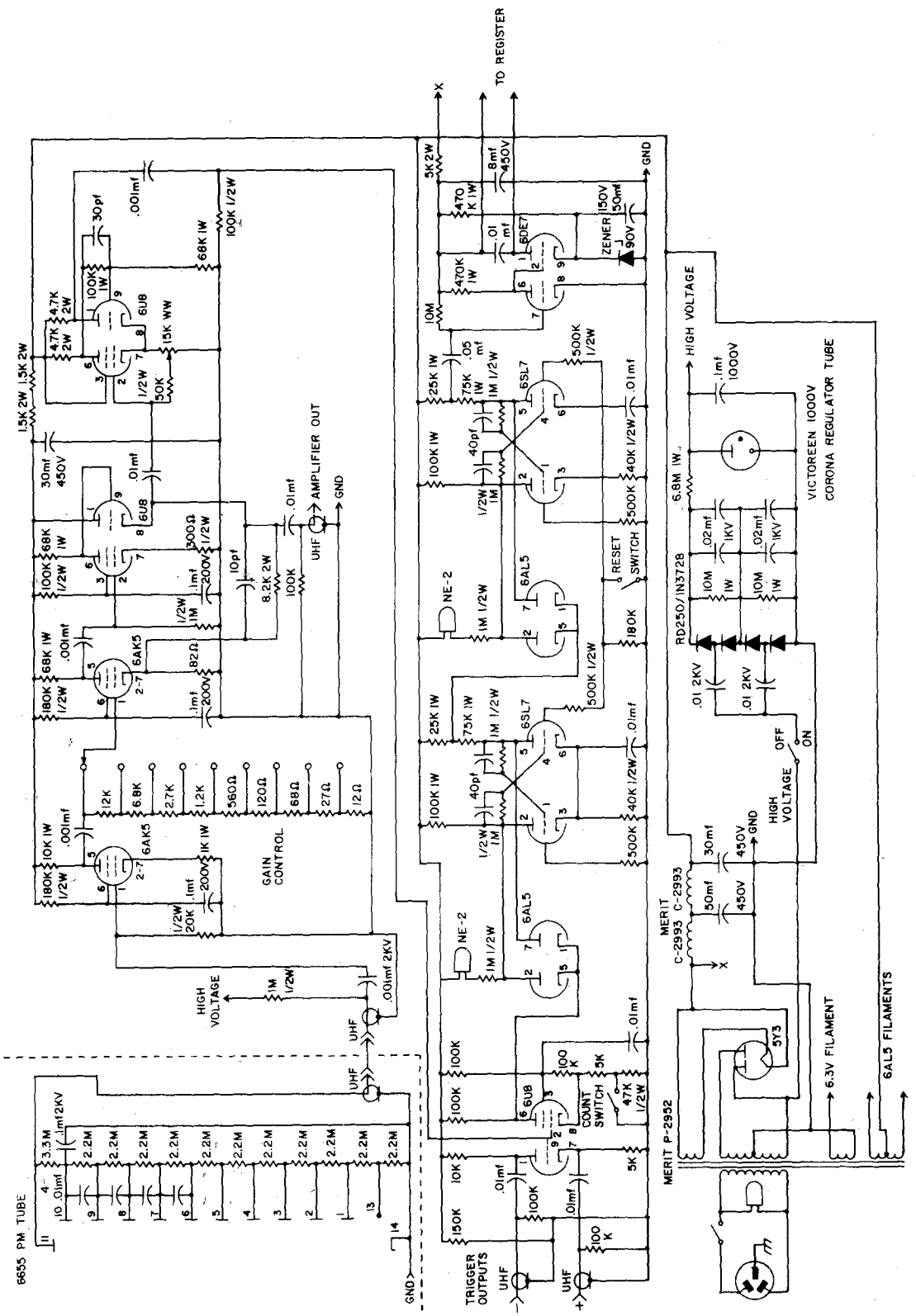


FIG. 1. Schematic diagram of the detector circuit.

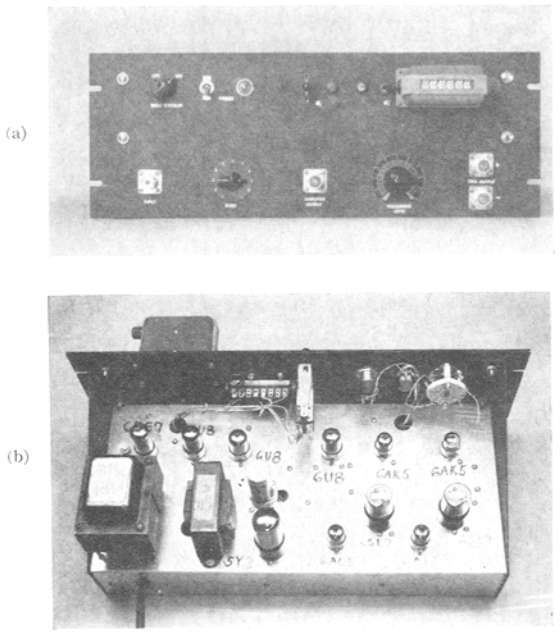

FIG. 2. Front and top views of the detector chassis.

discriminator plays an essential role in the analysis procedure which is described later. Positive and negative trigger signals derived from the discriminator output are available to aid in displaying the pulses counted on an auxiliary oscilloscope.

The binary scale of four was included mainly for pedagogic reasons; its use is not necessary for the rates normally encountered in the Rutherford scattering experiment. On the other hand, if use of the scintillation counter in other experiments is envisioned, it would probably be worthwhile to provide more binary stages than indicated. The output of the electronic scaler activates an electromechanical register. The photomultiplier high-voltage supply consists of a quadrupler circuit whose input was taken from the power transformer; the high-voltage output (1000 V) is regulated by a gas-discharge tube.

Figures 3 and 4 show how the original design of the cage holding source and foil was modified to accommodate interchangeable foil holders. This allows scattering measurements to be made on more than one element (nickel and gold foils are used), but a more important reason for introducing the change was to permit the evaluation of background effects on the basis of foil-out rates measured with an empty foil holder.

The insert indicated in Fig. 3 can be used to decrease the minimum scattering angle from 27° to 23° by increasing the length of the cage. Although this angular change is small, it corresponds to a significant change (a factor of two) in differential scattering cross section. Also, the use of the extension provides an opportunity for students to demonstrate that the measured differential scattering cross section does not depend upon the geometry of the apparatus.

## THE EXPERIMENT

The purpose of the following discussion, which is based on an instruction sheet handed out to students, is to explain how the apparatus described above may be used to obtain quantitative data on Rutherford scattering. Familiarity with the basic features of the MIT unit is assumed but, for ease of reference, Fig. 5 adapted from the ADP writeup has been included to show the annular geometry of source, scattering foil, and detector.

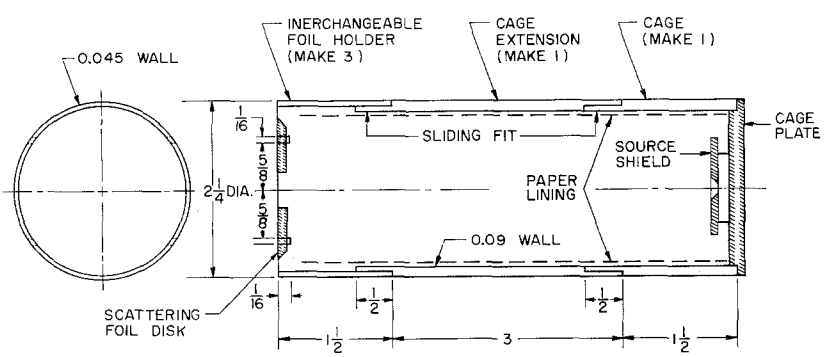


FIG. 3. Construction drawing of modified source cage and foil holder. Shaded parts are the same as in the original ADP design.

The object of the experiment is to measure, as a function of scattering angle $\theta$, the differential scattering cross section which is given by the equation

$$\frac{d\sigma}{d\Omega}=\frac{\text{Number of scattered } \alpha \text{ particles detected per second}}{\begin{array}{lll}\text{Total number of atoms in the foil} & \text{Number of } \alpha \text{ particles incident on the foil per second per cm}^2 & \text{The solid angle subtended by the detector at the foil.}\end{array}}$$

The quantities appearing here are determined as follows.

The number of alpha particles incident on the foil per cm$^2$/sec is obtained by allowing the alpha particles to pass directly to the detector through a small hole of known area which can be placed at the center of the foil ring. This is done with the scattering foil covered. The alpha flux striking the foil is given by

$$\frac{\text{Number of } \alpha \text{ particles detected per sec with hole open}}{\text{Area of hole}}\cdot\frac{(\text{Distance from source to hole})^2}{(\text{Distance from source to foil})^2}\cdot\cos\theta_S.$$

The total number of atoms in the foil can be found by weighing a sample of similar foil of known area

$$N(\text{Total})=\text{Area of foil (cm}^2)\cdot\text{Number of layers}\cdot\frac{\text{Weight of sample (g)}}{\text{Area of sample (cm}^2)}\cdot\frac{\text{Avogadro's number}\ \left(\frac{\text{atoms}}{\text{mole}}\right)}{\text{Atomic weight of foil}\ \left(\frac{\text{g}}{\text{mole}}\right)}.$$

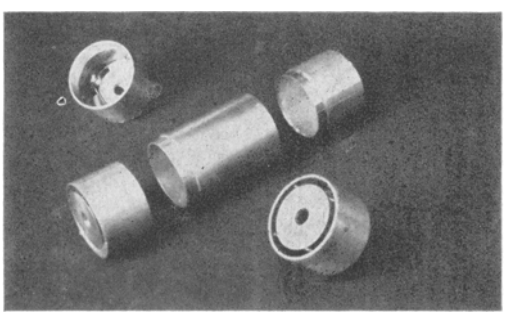

FIG. 4. Photograph of modified cage and foil holders. Normally, the foil holder is placed directly on the cage; but, if desired, the extension can be placed between holder and cage.

The solid angle subtended by the detector at the foil is given by

$$\Delta\Omega=[A_D/(d^2+r^2)]\cos\theta_D,$$

where $d$ and $\theta_D$ are defined in Fig. 5 and $A_D$ is the area of the detector. $r=\frac{1}{2}(r_1+r_2)$ is the mean radius of the foil ring.

The scattering angle $\theta$ is the sum of the two angles $\theta_S$ and $\theta_D$ appearing in Fig. 5. These can be obtained from the geometry:

$$\tan\theta_S=r/l;\quad \tan\theta_D=r/d.$$

The number of scattered alpha particles detected per second is obtained from the observed counting rates, but the procedure for doing this involves more than simply noting the counting rate of the detector. Complications arise in finding an appropriate value for the minimum pulse height, which is allowed to activate the counter. This minimum pulse height, which is determined by the setting of the discriminator triggering level, must be chosen very carefully in order to avoid certain spurious effects due to energy loss of the alpha particles in the foil and due to scattering of alpha particles from the walls of the chamber and foil holder. For reasons which will become apparent, it is helpful in finding a suit-

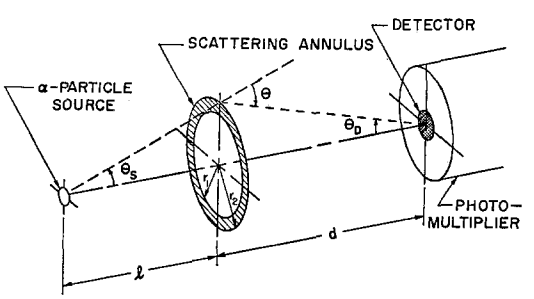


FIG. 5. Geometry of the experiment.

able triggering level to make graphs of observed counting rate vs the triggering level or "bias." Such graphs, which are commonly called "bias curves," can be interpreted as pulse-height spectra and can be used to discriminate between alpha particles of different energies.

In taking data for bias curves, students are instructed to save time by counting for the minimum period required to define the curves with reasonable statistical accuracy. For most of the curves called for, conditions are such that 100 counts ($\pm 10\%$ accuracy) can be accumulated in 10 or 15 sec. Bias curves are plotted as the data is taken so that results, which may affect the next step in the experiment, are immediately available.

To become familiar with the apparatus and with the interpretation of bias curves, students start the experiment by studying alpha particles coming through the hole (with the scattering foil covered). Figure 6 shows bias curves that might typically be obtained in this configuration. If all of the alpha pulses should have exactly the same height, a counting rate equal to the rate at which alphas hit the detector is recorded for all triggering levels less than that corresponding to the height; for all triggering levels greater than this, no counts are recorded. This behavior is illustrated by the "ideal" curve of Fig. 6.

Curve 1 which is a fair approximation to the ideal behavior illustrates what might actually be observed if the particles are allowed to go directly from source to detector without having to penetrate any matter. The sharp discontinuity or "edge" is smeared out because the pulse heights are distributed over a finite range and there is a sharp increase in rate at low levels due to extraneous noise pulses. Nevertheless, the plateau between these regions is well defined and the rate here is equal to the rate at which particles are incident.

Curve 2 might be obtained if the small hole is covered with foil so that detected alpha particles have to penetrate the same thickness of foil that is to be used later in the scattering measurements. Here the leftward shift of the "edge" is a measure of the energy loss in the foil and further deterioration in the shape of the bias curve is evident. Although the slope of the plateau is appreciable, the rate observed at the same triggering level used in the scattering measurements is a well-defined quantity which can be used to determine the number of alpha particles incident on the foil per cm$^2$ per sec. The optimum setting of the triggering level control is to be determined later.

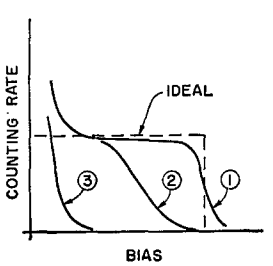


FIG. 6. Bias curves obtained for unscattered particles. See text for explanation.

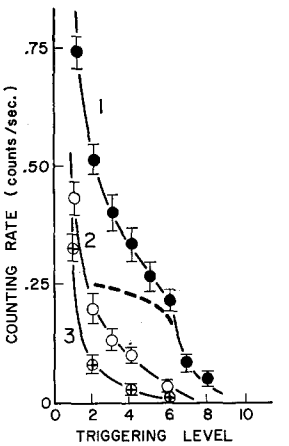


FIG. 7. Bias curves for scattered particles. See text for explanation.

Curve 3 indicates the shape of bias curves obtained when the chamber is filled with air at atmospheric pressure or when the hole is covered with tape so that particles from the source are prevented from reaching the detector. Under either of these conditions, only the pulses due to noise or background radioactivity should be present and the two curves should be identical. Any significant differences are an indication of contamination of the chamber walls by material leaking from the source. These curves are a background rate which should be subtracted whenever accurate values are to be read off bias curves.

It is worth noting here that the phenomenon of energy loss by ionization illustrated by the curves of Fig. 6 is, in itself, an appropriate subject for an advanced laboratory experiment. It would require only minor modifications to adapt the present apparatus for such an experiment.

After the preliminary measurements described above are completed, the students obtain bias curves for scattered particles such as those illustrated in Fig. 7. Curve 1 was obtained with a gold scattering foil while Curve 2 was obtained with

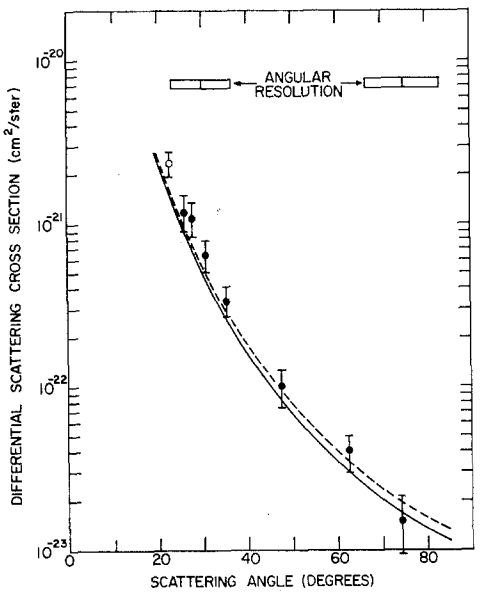


FIG. 8. Comparison of experimental results with theoretical curves. The dashed curve indicates the effect of finite angular resolution on the results. Note that the cross section measured at 23° with the cage extension in place (open circle) is consistent with the other data.

the dummy holder in place; the dotted line representing the difference between these curves exhibits a well-defined plateau whose rate is a valid measure of the intensity of alpha particles scattered by the foil. Note that the rate at which scattered alphas strike the detector cannot be determined from Curve 1 alone because, in the absence of a plateau, there is no valid criterion for deciding upon a suitable setting for the threshold. Some of the pulses observed in the absence of a scattering foil (Curve 2) come from background effects mentioned earlier, but most of them are due to alpha particles scattered from the brass walls of the cage and vacuum chamber. Curve 3, which was obtained with these walls covered with paper, confirms this interpretation; the difference between it and Curve 2 reflects the fact that scattering by paper—whose atomic number is relatively small—is less than by brass. The effects of wall scattering can be minimized by leaving the paper lining permanently in place during the final scattering measurements, but it is instructive for students to plot and to interpret curves similar to those of Fig. 7.

In principle, a plateau rate based on detailed curves similar to those of Fig. 7 should be obtained for each angle studied. In practice, detailed curves for only one angle provide a basis for choosing a fixed operating bias to be used for the final measurements of scattered particle intensity vs angle and for the determination of incident flux from the bias curves of Fig. 6. This operating level should lie on the plateau defined by the dotted difference curve of Fig. 7; it should be far enough below the "edge" so that most of the scattered alphas are counted but not so far below that the background rate is large compared to the plateau rate. When the bias has been set at a suitable operating level, the number of scattered alpha particles detected per second (the basic quantity appearing in the expression for the cross section) is given with sufficient accuracy by the difference between the rate observed with the foil in place and the background rate observed with an empty foil holder.

In Fig. 8, experimental points obtained by following the above procedure are compared with calculated cross sections based on the Rutherford formula (solid curve). Perfect agreement with the calculated curve is not to be expected *a priori* because each experimental point actually represents a summation over a fairly large range of scattering angles. The effect of this finite angular resolution is indicated by the dashed curve which was obtained by "folding" into the theoretical curve an approximate angular resolution function graphically constructed with the aid of a drawing of the apparatus. Even though the angular spread (indicated by bars at the top of Fig. 8) is quite large, the resulting deviation from calculated values is small and is, in fact, comparable to the statistical dispersion of the experimental points. It should be noted that the excellent agreement with theory displayed in Fig. 8 was obtained with an alpha particle energy corrected for the energy loss in the foil as determined from the bias curves of Fig. 6.

The results illustrated in Fig. 8 are convincing if not precise; agreement to 20% between experiment and theory is typically obtained by students. A further important aspect of the exercise is that it gives students some of the flavor of "real" experiments in which extensive auxiliary measurements aimed at obtaining a better understanding of the apparatus are usually necessary before valid conclusions can be drawn.

## ACKNOWLEDGMENTS

The author would like to thank Richard Boyd and Eric Becklin for their help in setting up and testing the experiment.